

# Microclimatic conditions in Ingá Park – Maringá (Paraná, Brazil) according to air humidity parameters

Cíntia Minaki<sup>1</sup> 

Vincent Dubreuil<sup>2</sup> 

Margarete Cristiane de Costa Trindade Amorim<sup>3</sup> 

## Keywords:

Maringá-PR  
Precipitable water  
vapor MSI/Sentinel-2A  
Climatological Station  
Simepar

## Abstract

The complexity of measuring water in its different physical states stems partially from inaccurate recording instruments and limited climatic parameters. As atmospheric composition is variable, researchers use several indexes to describe one of its elements, water vapor. The present research estimates air humidity in Ingá Park, in Maringá city, Paraná State, Brazil. For that, we used relative humidity data obtained from a temperature and humidity recorder inserted in the park. The data refer to the period from April 2019 to January 2020 and from June 2020 to March 2021. We also used remote sensing to verify the amount of precipitable water vapor over the same area in the available time interval of MSI/Sentinel 2A images. Ingá Park has the potential to improve beneficial effects to the city, especially considering the relative humidity and the condition of faster saturation of that observation station. According to the analysis of orbital images, precipitable water vapor in the park was 26,298 mm in 2019 and 25,950 mm in 2020, with a reduction in the first six months in the period from 2019 to 2021. Water vapor estimation through orbital images corroborated the data measured by the fixed sensor. Although these measurements are not equivalent, the study showed a decreasing dynamics of air humidity.

<sup>1</sup> Universidade Estadual de Maringá – UEM, Maringá, PR, Brazil. [cminaki@uem.br](mailto:cminaki@uem.br)

<sup>2</sup> Université Rennes 2 – Rennes, France. [vincent.dubreuil@univ-rennes2.fr](mailto:vincent.dubreuil@univ-rennes2.fr)

<sup>3</sup> Universidade Estadual Paulista – UNESP, Presidente Prudente, SP, Brazil. [margarete.amorim@unesp.br](mailto:margarete.amorim@unesp.br)

## INTRODUCTION

Water in the climate system is a difficult element to measure. This is because estimating it in its different physical states requires more accuracy than that achieved by recording instruments. In the gas phase, the physical and latitudinal diversity and the peculiarity of environments and water regimes demonstrate how water vapor is variable on time-space scales within the global hydrological cycle. Even with these particularities, it is essential to identify water dynamics in environments that require attention either for preservation or conservation in the case of protected units, or for awareness and monitoring in the case of occupied areas without a special regime of use, which can be used as scientific research targets.

Water vapor in the atmospheric reservoir emits much of the terrestrial infrared radiation into space from condensation of latent heat, formation of clouds, and production of rain (BARRY; CHORLEY, 2013, p. 79), regulating the weather and climate. The average storage of water vapor in the atmosphere is equivalent to the precipitable water content and corresponds to a 10-day supply of rain to the Earth (BARRY; CHORLEY, 2013, p. 79) in case all the vapor present condenses. Sutcliffe (1956) estimated this content to be 25 mm in January and 20 mm in July for the Southern Hemisphere. However, the horizontal influx of moisture into the air allows recorded rainfall values to be higher than this precipitable water content (BARRY; CHORLEY, 2013, p. 79). Therefore, this atmospheric storage is a small value in relation to the registered rainfall, to which the gains and losses of moisture or energy must be computed (SUTCLIFFE, 1956, p. 394).

Tuller (1968, p. 795-796) studied the global distribution of precipitable water between 1964 and 1966. The author reaffirms the already known distribution and emphasizes that the Southern Hemisphere has a more regular pattern of influence of latitude on precipitable water than the Northern Hemisphere, largely because of their differences in land and water distribution.

The impacts of abundance or scarcity of water vapor on the weather and climate arise great interest in measuring this variable in the surface air (Integrated Water Vapor - IWV) or in a vertical column above the atmosphere (precipitable water or height of an equivalent column of liquid water on the surface - WVP) (MAGHRABI; DAJANI, 2013, p. 2).

A common way to quantify humidity disregarding partial and saturated water vapor pressure is to describe the amount of water vapor present in the atmosphere (WALLACE; HOBBS, 2006, p. 80-83) from indexes that represent its content. These include absolute humidity, specific humidity, relative humidity, and dew point temperature (WALLACE; HOBBS, 2006, p. 80-83; BARRY; CHORLEY, 2013, p. 80). Each index has forms of quantification that correlate with a degree of imprecision. This limitation is the main source of error in short-term precipitation forecasts such as 0- to 24-hour forecasts (BEVIS et al., 1992, p. 787).

The study of the source of water vapor in the different areas reveals how much water cycling is a mechanism that reduces the average storage of water vapor in the atmosphere when absent due to deforestation problems, fires, or even climate variability. This absence decreases the expectation of water transport between regions, interfering with regional atmospheric circulation and seasonal transport, which are usually stable in tropical latitudes (SUTCLIFFE, 1956).

The present research addressed atmospheric humidity, commonly considered as water vapor. The study was developed in Maringá city, Paraná State, Brazil, covering the urban area of Ingá Park. Considering that air humidity depends on one or more elements such as those mentioned above, we estimated this variable in Ingá Park by more than one means and by more than one index. Therefore, we analyzed relative humidity data recorded by a temperature and humidity sensor inserted in the park. The data refer to the period from April 2019 to January 2020 and from June 2020 to March 2021. These periods correspond to the total data available within the park, and cover different seasons.

Furthermore, we used orbital images to verify the amount of precipitable water vapor in an air column over the park area. The available time interval of these images covers the period from December 2018 to July 2021. The hypothesis is that Ingá Park has microclimatic conditions associated with air humidity that favor the urban environment more than the regions of fixed meteorological stations that will be used as a parameter. This is because the park is a conservation unit, and these meteorological stations are located in areas whose vegetation has been removed since the beginning of urban occupation.

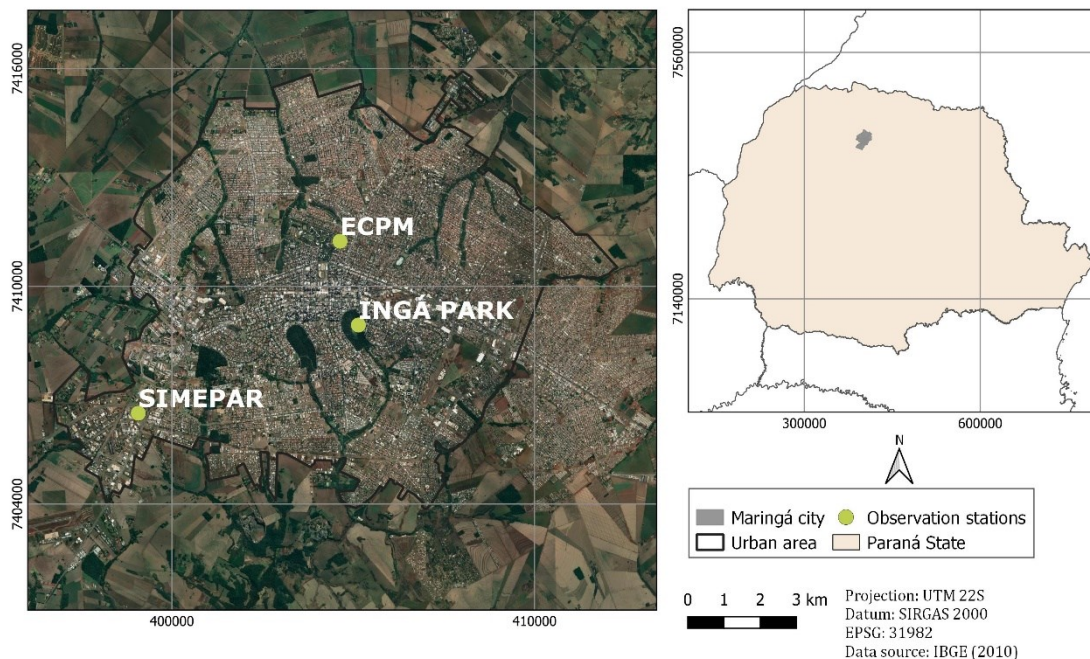
## MATERIALS AND METHODS

### Study Site

Maringá city is located in the north-central mesoregion of Paraná State, Brazil (IBGE, 1990, p. 105-106). It is a medium-sized city with an estimated population of 436,472 inhabitants (IBGE, 2021). The climate of the area is characterized by the transition between tropical and subtropical types (MINAKI,

MONTANHER, 2019). This is due to its latitudinal location on the 23°S parallel, being thus under the influence of tropical and extratropical atmospheric systems (Figure 1). Dubreuil et al. (2015) studied the frequency of annual climate types for Maringá according to the Köppen classification, reaching the following results for the period from 1961 to 2015: 44% - Aw, 16% - Am, 22% - Cwa, 13% - Cfa, and 5% - Csa. The incidence of the different climatic groups “A” and “C” reinforce the characteristics of transition and variability of the area.

Figure 1 - Location of Maringá city, Paraná State, and observation stations used in the research.



Source: The authors (2021).

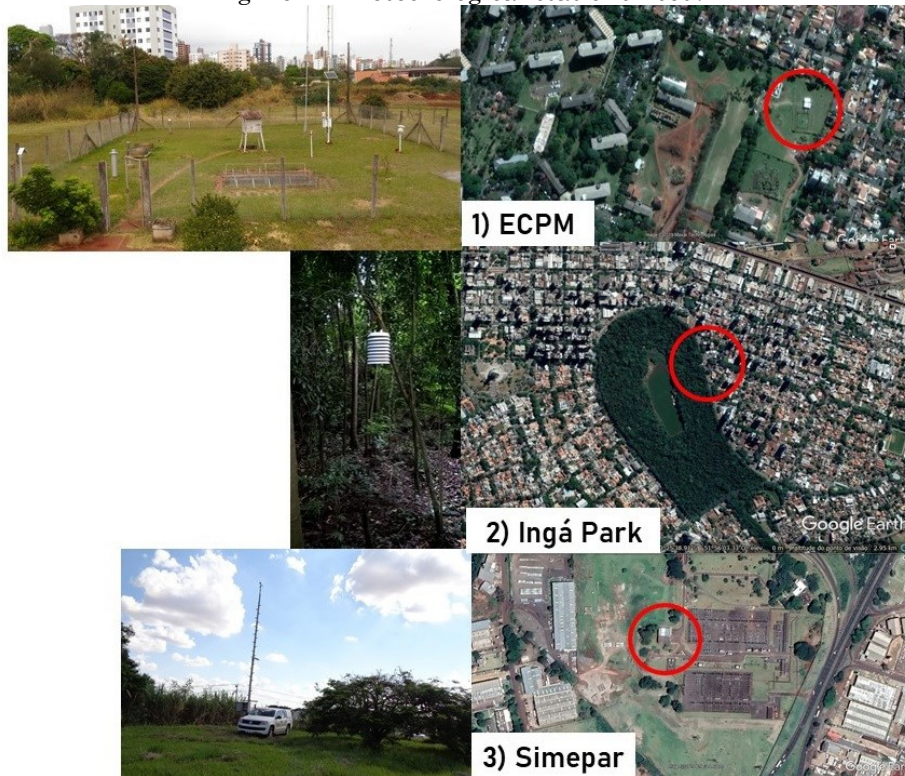
Maringá has an area of 487,012 km<sup>2</sup>. Since its foundation in 1951 it has experienced urban and demographic growth, mainly until the 1980s (RESCHILIAN; UEHARA, 2012, p. 79). The result was an increase in infrastructure and buildings, and a reduction in vegetation cover to the benefit of buildings.

The city has two surface meteorological stations which will be used as references due to the observation networks to which they belong and the extent of their data series. The Estação Climatológica Principal de Maringá (ECPM), climatological station belongs to the category of the most complete stations (VIANELLO; ALVES, 2012, p. 284), enabling long-term studies. It is part of the network of the Instituto Nacional de Meteorologia (INMET), specific federal government agency, belonging to the global meteorological system. The station code

in the World Meteorological Organization (WMO) network is 83767. The other station is an automatic meteorological station (VIANELLO; ALVES, 2012, p. 286) belonging to the Sistema de Tecnologia e Monitoramento Ambiental do Paraná (Simepar), entity governed by private law and public interest, which has approximately 50 stations in the state, and will be called Automatic Meteorological Station (EMA).

Station ECPM is the one that holds the largest historical series (from 1980 to 2021), covering complete calendar years since it was installed inside the State University of Maringá (UEM), which is a public university in the state of Paraná. Figure 1 shows the location of the stations and Figure 2 shows the characteristics of each environment.

Figure 2 – Meteorological stations used.



Source: The authors (2021); Simepar (2021).

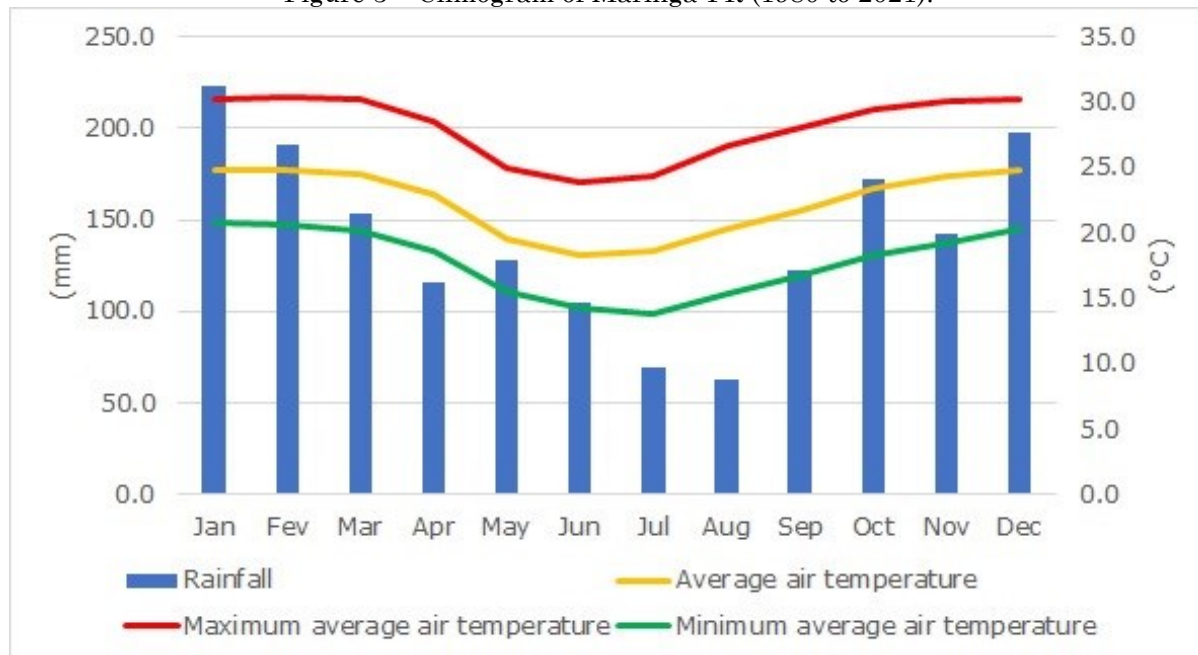
Station ECPM is located in the north-central portion of Maringá. It is covered by a hedge of undergrowth and surrounded by houses. Ingá Park is located in the central area, and the thermal-hygrometric recorder is covered by trees, standing over mulch-covered soil. The EMA of Simepar is located in the southwest portion of Maringá, in a place with low and medium-sized vegetation. The area is close to industrial occupation and state highways (Figure 2).

Ingá Park is a conservation unit currently classified as an Área de Relevante Interesse Ecológico (ARIE) (BRASIL, 2000; MARINGÁ, 2016), a category of federal Conservation Unit.

It was created by Ordinary Law No. 880/1971 and covers an area of 51 ha (MARINGÁ, 1971). Since its formation it has undergone changes in infrastructure, service supply, and population access to the place. Relative humidity data for this area come from the *in situ* installation of a thermohygrometer, which will be described in section 2.2.

According to the largest historical series among the reference stations (ECPM, 1980 to 2021), Maringá has an average rainfall of 1682.3 mm and an average annual temperature of 22.3 °C (Figure 3).

Figure 3 – Climogram of Maringá-PR (1980 to 2021).



Data source: INMET (2021).

Figure 3 shows that spring-summer is the wettest period. In autumn-winter it rains approximately 60% of the volume of spring-summer. Minaki and Montanher (2020, p. 530-532) studied this region by using a data series from 2002 to 2019. According to these authors, Maringá does not have a pattern of rainfall seasonality although its interannual variability points to the existence of dry periods. Thermal amplitudes (annual average, minimum average,

and maximum average) between spring and summer are 5.7 °C, 6.1 °C, and 5.3 °C, respectively, in which the influence of continentality stands out.

The use of three observation stations makes it possible to highlight the microclimatic characteristics expected at the park level, given its physical configuration and distinct landscape. Table 1 provides an overall description of the observation stations.

**Table 1** – Characteristics of the observation stations.

Station	Coordinates	Altitude (m)	Location
ECPM	23°25' S; 51°57' W	542	North-central
Simepar	23°26' S; 51°59' W	570	Southwest
Ingá Park	23°25' S; 51°55' W	539	Central

Data source: The authors (2021).

### Methodological procedures

As the objective was to estimate air humidity in Ingá Park by more than one means and by more than one index, the methodological procedures will be described in two stages.

The first step consisted of evaluating relative humidity in the periods from 2019 to 2021 by using data released by INMET and Simepar as well as measurements from a temperature and humidity data recorder installed inside the park. The installation of this recorder followed the instructions of the World Meteorological Organization (WMO, 2008). The ThermaData Humidity – Temperature Logger, model HTD, brand ETI (Electronic Temperature Instruments) was protected in an Ambient

Weather SRS 100 Pagoda Temperature and Humidity Radiation Shield. Hourly data were recorded on air temperature and relative humidity in two periods, from April 2019 to January 2020 (first period) and from June 2020 to March 2021 (second period), totaling the 14,640 data for each variable.

Considering the three stations and the two data periods, the first step consisted of: i) analyzing the association between air temperature and relative air humidity by using Pearson's linear correlation; ii) comparing average data; iii) applying the thermal discomfort index (TDI). The rationale for the correlation coefficient can be found in Morettin and Bussab (2013, p. 86-89).

In both periods the two reference stations had problems with missing data for the two variables. In ECPM, the failure covered the months of April and May 2020, corresponding to 10% of the total data. In Simepar, failures covered 0.8% of the total data, occurring in November 2019. Although Brubacher et al. (2020, p. 340-341) proved that the efficiency of methodologies increases with the increase in the number of stations used, data were not filled in given the difficulty in obtaining satisfactory results on the daily scale (MELLO et al., 2017, p. 120). No procedure was tested for Maringá due to the extreme events and the variability of rainfall and temperature in the city. Statistical analyses were performed using the R program (R CORE TEAM, 2020).

With a view to contribute to the assumption of the beneficial effects of the park on the urban environment, the thermal discomfort index (TDI) proposed by Kawamura (1965 apud ONO; KAWAMURA, 1991) was applied. This TDI is similar to that of Thom (1959) and uses dry bulb temperature and dew point temperature (Equation 1). When estimating thermal comfort (discomfort) in an area through a formula, it is noteworthy that some climatic variables tend to overlap, excluding others from the analysis.

$$DI = 0.99T + 0.36 T_{dp} + 41.5 \text{ (Equation 1)}$$

Where:

$DI$  = Thermal discomfort index

$T$  = Temperature value in °C

$T_{dp}$  = Dew point temperature in °C

The second stage of the analysis consisted of assessing air humidity in Ingá Park through satellite images available on the Google Earth Engine (GEE) geospatial analysis platform. The selected band of the Sentinel-2 satellite, level 2A, does not allow the detection of relative air humidity, but rather of a measure of atmospheric water vapor. The product used is called WVP (Water Vapor Pressure), which will be referred to as the WVP band. It is the result of an estimate that mainly considers band 9 of the Multispectral Imager (MSI) sensor and radiative transfer models.

The WVP band is the height that water would occupy in an air column if the vapor were to condense (ESA, 2021). The band does not have such a common application in humidity studies, but has the potential to contribute to an integrated analysis such as the one proposed here.

All available data from the WVP band spanning from December 2018 to July 2021 were used, totaling 182 Sentinel-2A images. Regarding the satellite passage, the temporal interval of 5 days prevailed. However, this interval was not constant; in some moments, the frequency of images ranged from 10 to 15 days. The Sentinel mission started in 2014, being operated by the European Space Agency (ESA). Sentinel-2A was launched in 2015 (EMBRAPA, 2021).

The WVP band has a 10-m spatial resolution (originally 20 m, being resampled and made available at 10 m) and was used to extract an average value for Ingá Park. For that, the park boundary was vectorized, and from this polygon an internal buffer was applied with a linear distance equivalent to the spatial resolution of the WVP band. The buffer polygon was used to calculate the averages. It is noteworthy that the use of the WVP band of Sentinel-2A images has as its main advantage the possibility of extracting average estimates for the park area, extrapolating punctual analysis. The 182 images were processed using JavaScript programming lines.

## RESULTS AND DISCUSSION

### *First step - Analysis of relative air humidity in the observation stations*

According to the data generated by Pearson's linear correlation, the greatest association between temperature and relative humidity occurred in the second period (Table 2). This can be explained by the synoptic conditions prevailing at the time, although the results are close. In both periods, Simepar obtained the highest R value; in the first case, the confidence interval also covered the R value of the park. Overall, ECPM had the lowest correlation. Although the other two stations had an increased correlation in the second period, the correlation of ECPM decreased in that period in relation to the first period.

The surroundings of ECPM, even inside the University, have undergone changes in recent years. This has intensified the loss of standardization of installation aspects in the same way as happens with most meteorological stations in the country. The increase in buildings, the reduction of permeable surfaces, and the increase in the flow of people and cars interfere and diversify the dynamics of the climatic elements in the place.

**Table 2** – Results of Pearson's linear correlation between air temperature and relative air humidity.

1 <sup>st</sup> period (April 2019 to January 2020)			
Reference Station	P-value	R	IC (95%)
Ingá Park	<2.2.10 <sup>-16</sup>	-0.5669	-0.5822 to -0.5512
Simepar	<2.2.10 <sup>-16</sup>	-0.5764	-0.5916 to -0.5608
ECPM	<2.2.10 <sup>-16</sup>	-0.5475	-0.5626 to -0.5320
2 <sup>nd</sup> period (June 2020 to March 2021)			
Ingá Park	<2.2.10 <sup>-16</sup>	-0.6481	-0.6612 to -0.6346
Simepar	<2.2.10 <sup>-16</sup>	-0.6780	-0.6902 to -0.6654
ECPM	<2.2.10 <sup>-16</sup>	-0.5216	-0.5990 to -0.4346

Source: The authors (2021).

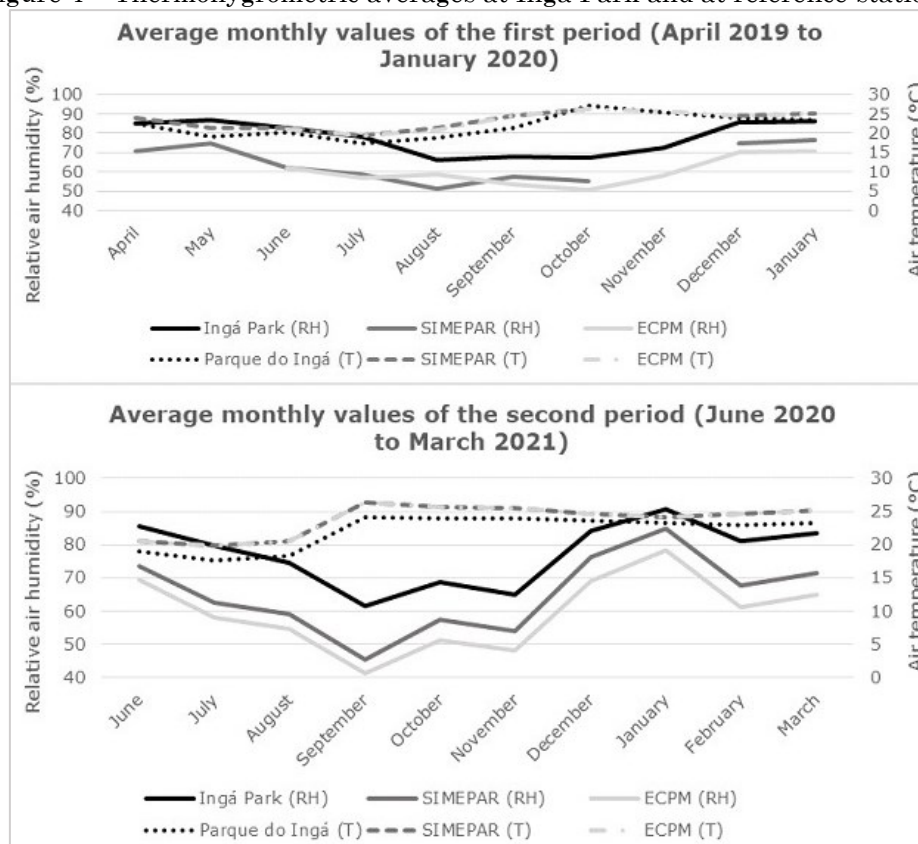
Regarding the aspect of negative correlation, under normal conditions of stability, the lower the air temperature the higher the relative humidity tends to be and vice versa. Under conditions of instability, the atmosphere is subject to variations that do not necessarily follow a linear pattern.

The low value of  $\rho$  ( $\rho < \alpha$ ) observed in all stations indicates the statistical significance of the variable temperature in relation to relative air humidity, showing that the correlations differ from zero. Many factors can influence temperature, such as solar radiation, terrestrial albedo, altitude, air mixture, heat loss by evaporation of water (RANSOM, 1963, p. 23),

rainfall, among others. These are the reasons for the correlations not to be close to 1.

The comparative analysis of the averages between the stations shows an opposite configuration of the lines of the two elements (Figure 4). Ingá Park, which had the lowest temperature, recorded higher values of relative humidity, the opposite occurring with the other two stations. In the first period, the highest thermal average of Simepar differed from the lowest thermal average of ECPM by 0.9°C. In the second period, the average temperature was equal between both stations and rose to 23.7 °C. In that same period, the record of relative humidity was almost equivalent.

Figure 4 – Thermohygrometric averages at Ingá Park and at reference stations.



Data source: INMET (2021) and Simepar (2021).

\*As reported in section 2.2, there were missing data from EMA Simepar in November 2020 and from ECPM in April and May 2019.

Regarding data from Ingá Park, in the first period, the month of May had the highest average relative humidity, followed by January and December. The averages gradually decreased from June to August (mostly winter months), mainly for ECPM and Simepar, increasing again in September. In the second period, the month with the highest hygrometric average was January, followed by June and December, and the average values decreased for all stations, mainly from September to November.

In both periods, the lower relative humidity between winter and spring contributed to the reduction of rainfall. Station ECPM recorded a rainfall of 1424.2 mm in the year 2019, and 1296.2 mm in the year 2020. More than 79% of the 2019-2020 months had rainfall values below the climatology of the area.

With the predominance of rainfall deficit, rainfall was below at least one standard deviation from its mean for several months. According to INMET (2020), the non-configuration of the El Niño-Southern Oscillation (ENSO) in the period was decisive for the spatial and temporal irregularity of rainfall in the southern region of Brazil.

Meteorological combinations verified since November 2019 also favored the driest period in Maringá city, characterized by intense anticyclonic circulation generating air subsidence and decreasing rainfall in spring-summer. Moreover, the Front Systems and the South Atlantic Convergence Zone (SACZ), responsible for large volumes of rainfall at this time of year, were not so active. The variability

of atmospheric systems influenced the amount of water vapor incident on the area.

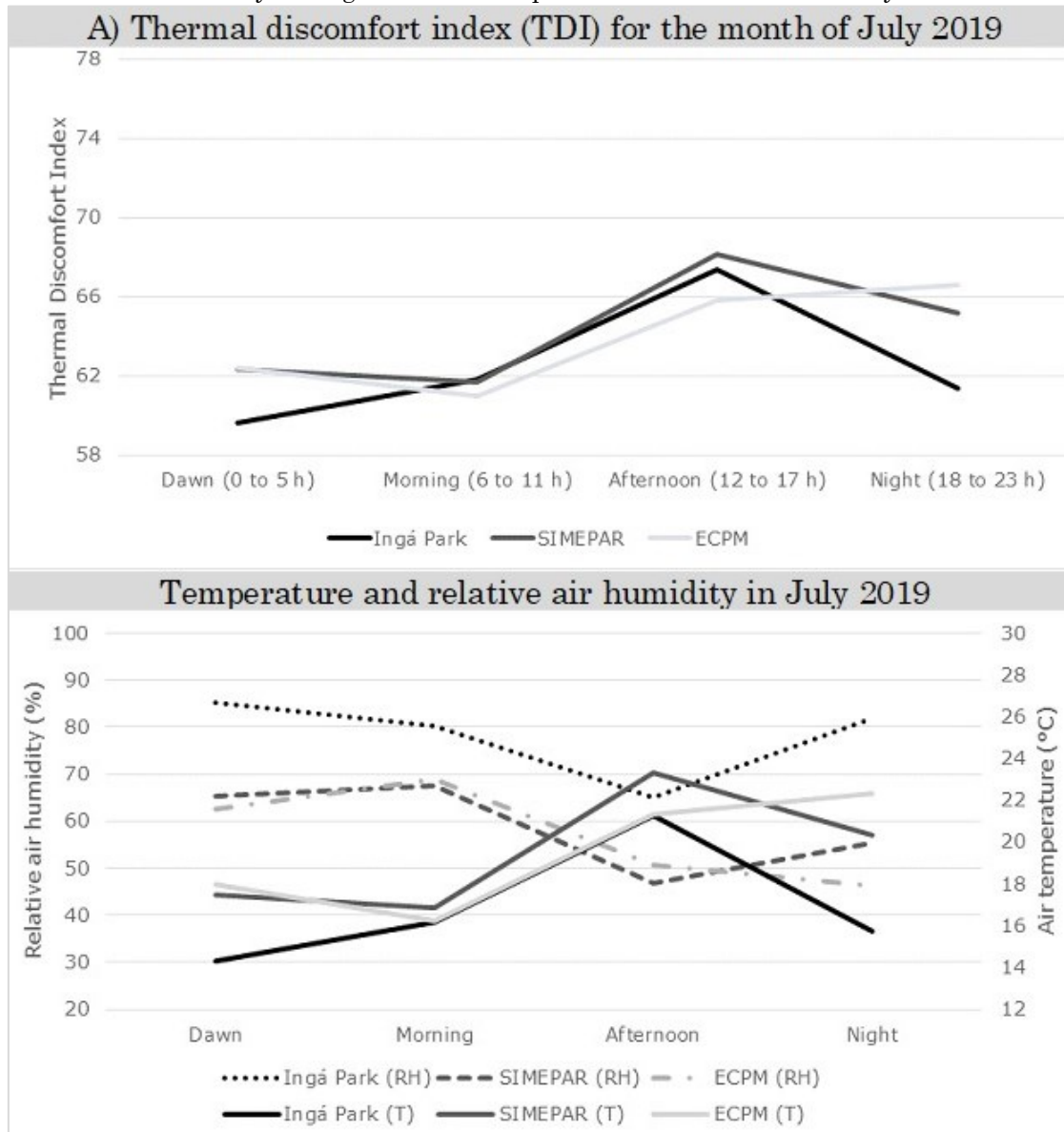
Between the first and second periods, the decrease in relative humidity and the increase in temperature were smaller in Ingá Park. For relative humidity, the decrease was 0.4% in the park and 0.5% in ECPM, while Simepar had an increase of 0.6%. The temperature increment was 0.1 °C in the park, 0.3 °C in ECPM, and 0.6 °C in Simepar. The average thermal and hygrometric records of Simepar between one period and another did not influence the inversely proportional relationship between temperature and relative humidity in January 2021.

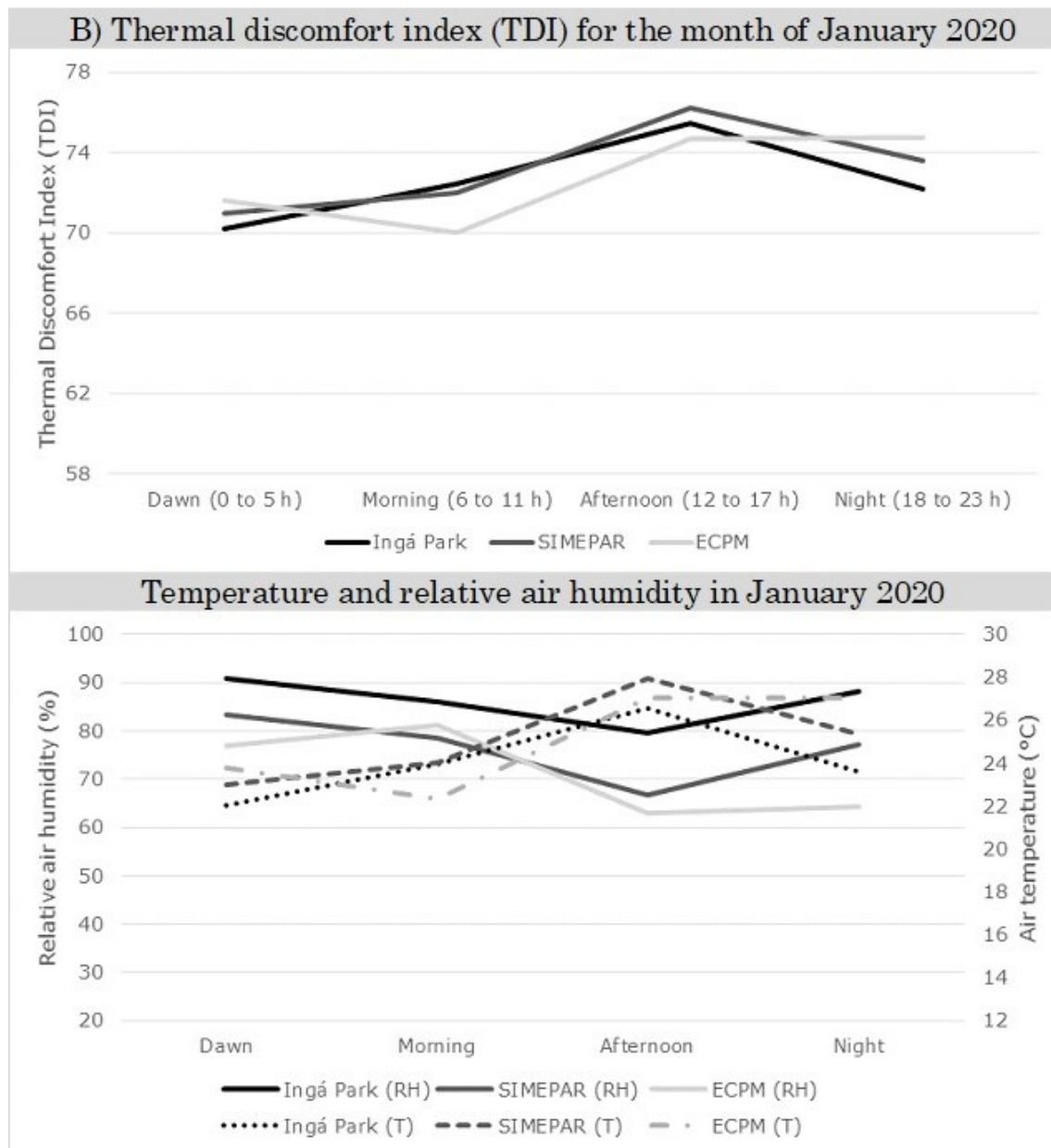
In the first period, with the exception of October, the park recorded the lowest average monthly temperatures, and in all months it had the highest average relative humidity.

In the second period, without exception, the park was the coolest and most humid place. The relative humidity values of Simepar and ECPM were close to each other, but always lower than the values measured in the park.

The record of higher relative humidity in the two periods for Ingá Park contributed to the lowest DTI in this area (Figure 5). The park area tends to mitigate the effects of problems common to the city (even though it is part of the city), that is, intense deforestation for waterproofing and construction; suppression of trees; and materials used in buildings, often with high absorption of solar radiation and low reflection. This mitigation occurs precisely because the area has characteristics opposite to what is relatively uniform in its surroundings.

Figure 5 - Thermal discomfort index (TDI) for the months of July 2019 and January 2020, and monthly average values of temperature and relative humidity.





Source: The authors (2021).

In both months (Figures 5A and 5B), Ingá Park recorded the lowest TDI during the night and dawn, that is, from 18:00 to 05:00 h.

The month of January 2020 stood out for the highest TDI as expected since it is a hotter month. However, the month of July accounted for the greatest thermal and hygrometric differences between the stations. In the morning, in January 2020, the park had the highest TDI, and ECPM the lowest. The low TDI of ECPM continued into the afternoon.

The higher TDI in the park in the morning suggests a great absorption of radiation by the vegetation in the warmer months. Notwithstanding, the area remained with the highest relative humidity, while the other stations had more temperature variation causing humidity variation.

In July 2019, Ingá Park accounted for the lowest temperature in all periods. Station ECPM recorded the highest temperatures during the night and dawn, while Simepar recorded the most extreme values during the morning and afternoon (Figure 5A). This month accounted for a greater thermal difference between the stations, reaching 6.5 °C at night.

The results of relative air humidity were inversely proportional to those of temperature. In July 2019, the park was wetter in all periods, especially at night and at dawn, with differences of up to 35%. During the day, the difference was smaller. Simepar stood out with the lowest humidity values during the day, while ECPM recorded the lowest values during the night and dawn.

In January 2020, the park was wetter in all periods, and ECPM was the least humid station not only during dawn and night, but also during the afternoon.

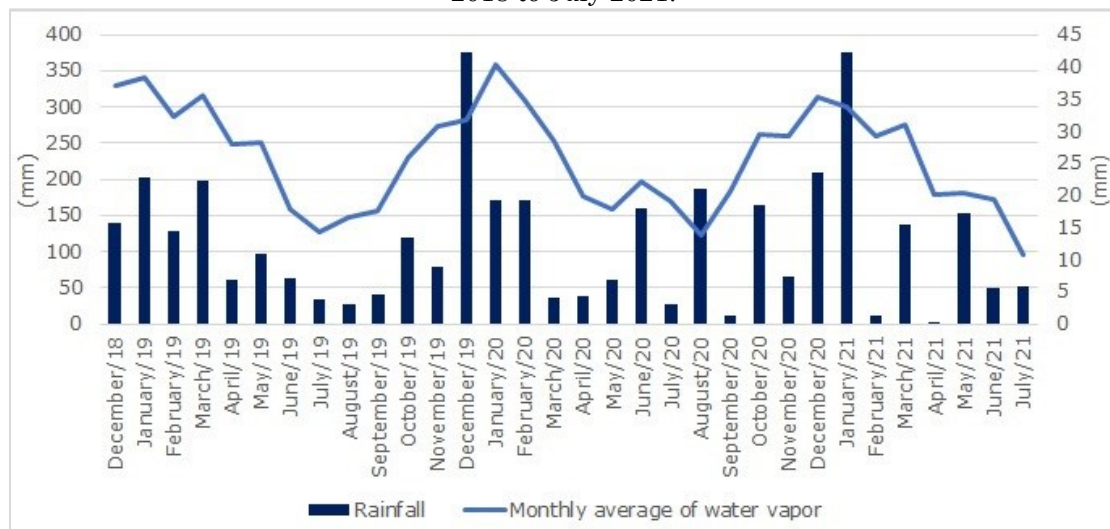
Overall, the highest thermal and hygrometric differences occurred at night, and the highest TDI in the afternoon. The stations used as parameters do not have the same vegetative characteristics or the same thermohygrometric control in the protected area, being more subject to the changes that

occur in their surroundings due to urban growth.

### *Second step - Estimation of water vapor in the air column over the park area*

The information obtained by processing Sentinel-2A images made it possible to estimate the water vapor in the air column over the park area at different periods (Figure 6).

Figure 6 - Average water vapor in the air column over Ingá Park and rainfall values from December 2018 to July 2021.



Data source: Water vapor: GHG/Sentinel 2A; rainfall: INMET (2021).

The largest amount of precipitable water vapor occurred in January (2019 and 2020), December (2018 and 2020), March (2019), and February (2019 and 2020), which correspond to the wettest months in the historical series. The data on the amount of precipitable water vapor and rainfall corroborate each other without being equivalent (Figure 6). Their dynamics is similar, with the exception that the total estimated water vapor cannot be interpreted only from rainfall values. As an example, the months of July and August stand out with the lowest values of precipitable water vapor, while the lowest values of rainfall extended beyond July and August to the months of April, September, and February.

The last months under study (Figure 6) show a decrease mainly in water vapor. Evapotranspiration, not considered in this work, is another variable that influences humidity (BARRY; CHORLEY, 2013, p. 80) and may explain this decrease. Variation of the advective input, which correlates with atmospheric movements, is another modulator of water vapor (KASTENDEUCH et al., 2019).

The year 2019 had an average precipitable water vapor of 26,398 mm, while the year 2020 had an average of 25,950 mm. The year 2021 was not fully considered; thus, for comparison with previous measurements, the average of this index was calculated from January to June for 2019, 2020, and 2021. The results were, respectively, 30.029 mm, 27.255 mm, and 25.601 mm, showing a reduction in the short period of the series.

Overall, the impacts that the continuous reduction of atmospheric humidity can cause to environments interfere with the horizontal and vertical transport of moisture and consequently with microclimatic characteristics. In the case of Ingá Park, it reduces the benefits provided by the area, homogenizing it in relation to its surroundings.

Domingos (2008, p. 20) mentions both the increase in building density in urban areas and industrialization as conditions that have a degrading effect on urban microclimates. Ingá Park fits into the first condition, whose effect refers to the decharacterization of its microclimate.

As observed by the results obtained in the correlation presented for the three stations, air temperature is a factor that influences relative humidity. Apart from this variable, interpreting the precipitable water vapor over Ingá Park is a more complex designation. As mentioned above, evapotranspiration levels and the horizontal influx of moisture affect water vapor in the atmospheric system. The main agents of each process - solar radiation and vegetation for evapotranspiration, and meteorological systems for the horizontal influx - specify the different environments of the city, making it a non-homogeneous surface under the aspect of water vapor.

The surface characteristics of Ingá Park, such as the presence of a lake, permeable areas, and tree cover contribute to the lower removal of water vapor in the diurnal cycle, which can be maximized in places where these characteristics do not predominate.

## FINAL CONSIDERATIONS

The particularities of Ingá Park as a green area embedded in the urban perimeter resulted in high relative humidity values, proving the hypothesis of the study. Although the correlation between temperature and relative humidity was not high (showing that changes in other climatic elements can interfere with this association), it is significant. The lowest TDI of the park occurred with cooling during the night and dawn in the representative months of summer and winter. In the afternoon, all stations had an increase in TDI, regardless of the month, demonstrating that they are affected by urban turmoil.

In turn, the estimate of precipitable water vapor through orbital images corroborated the relative humidity data measured by the fixed sensor installed in the park. Although these are not equivalent measures, the study showed a dynamic reduction of both indexes.

## FUNDING SOURCE

The authors of this research are grateful for the financial support of CAPES (Coordenação de Aperfeiçoamento de Pessoal de Nível Superior; Project CAPES/COFECUB - Cities, climate and vegetation: modeling and environmental public policies - CAPES (AUXPE: 88881.191765/2018-01).

## ACKNOWLEDGEMENTS

The authors of this research are grateful for the financial support from CAPES/COFECUB Program (Project: Cities, climate and vegetation: modeling and environmental public policies - Process: 88881.191765/2018-01), to the Instituto Nacional de Meteorologia (INMET) and to Sistema de Tecnologia e Monitoramento Ambiental do Paraná (Simepar) for providing meteorological and/or climatic data.

## REFERENCES

- BARRY; R. G.; CHORLEY, R. J. **Atmosfera, tempo e clima**. Tradução: Ronaldo Cataldo Costa. 9. ed. Porto Alegre: Bookman, 2013.
- BEVIS, M.; BUSINGER, S.; HERRING, T. A.; ROCKEN, C.; ANTHES, R. A.; WARE, R. H. GPS Meteorology: remote sensing of atmospheric water vapor using the global positioning system. **Journal of Geophysical Research**, v. 97, n. D14, p. 787-801, 1992. <https://doi.org/10.1029/92JD01517>
- BRASIL. **Lei nº 9.985, de 18 de julho de 2000**. Available: [http://www.planalto.gov.br/ccivil\\_03/leis/19985.htm](http://www.planalto.gov.br/ccivil_03/leis/19985.htm). Access on: 12 July, 2021.
- BRUBACHER, J. P.; OLIVEIRA, G. G. de; GUASSELLI, L. A. Preenchimento de falhas em séries temporais de precipitação diária no Rio Grande do Sul. **Revista Brasileira de Meteorologia**, v. 35, n. 2, p. 335-344, 2020. <https://doi.org/10.1590/0102-7786352035>
- DOMINGOS, S.I.S. **Microclimatologia do município de Sintra com base em estações meteorológicas**. 2008. 89 f. Dissertação (Mestrado em Ciências Geofísicas – Especialização Meteorologia). Universidade de Lisboa, Lisboa, 2008. Available: <https://repositorio.ul.pt/handle/10451/1294>. Access on: 22 August, 2021.
- DUBREUIL, V.; FANTE, K. P.; PLANCHON, O.; SANT'ANNA NETO, J. L. Os tipos de climas anuais no Brasil: uma classificação de Köppen de 1961 a 2015. **Confins**, n. 37, 2018. <https://doi.org/10.4000/confins.15738>
- EMBRAPA - Empresa Brasileira de Pesquisa Agropecuária. **Missão Sentinel**. 2021. Available: <https://www.embrapa.br/satelites-de-monitoramento/missoes/sentinel>. Access on: 4 July, 2021.
- ESA. **Sentinel-2 Products Specification Document**. 2021. Available: <https://sentinel.esa.int/documents/247904/685>

- 211/sentinel-2-products-specification-document. Access on: 15 March, 2022.
- IBGE. **Divisão do Brasil em mesorregiões e microrregiões geográficas**. Rio de Janeiro: IBGE, 1990. 135 p. Available: [https://biblioteca.ibge.gov.br/visualizacao/monografias/GEBIS%20-%20RJ/DRB/Divisao%20regional\\_v01.pdf](https://biblioteca.ibge.gov.br/visualizacao/monografias/GEBIS%20-%20RJ/DRB/Divisao%20regional_v01.pdf). Access on: 8 August, 2017.
- IBGE. Cidades. Available: <https://cidades.ibge.gov.br/brasil/pr/maringa/p panorama>. Access on: 15 March, 2021.
- IBGE. Downloads. 2010. Available: [https://ftp.ibge.gov.br/Censos/Censo\\_Demografico\\_2010/Resultados\\_do\\_Universo/Agregados\\_por\\_Setores\\_Censitarios/](https://ftp.ibge.gov.br/Censos/Censo_Demografico_2010/Resultados_do_Universo/Agregados_por_Setores_Censitarios/). Access on: 19 December, 2021.
- INMET - Instituto Nacional de Meteorologia. **Prognóstico climático de outono**. 2020. Available: [http://www.inmet.gov.br/portal/notas\\_tecnicas/2020/prognostico\\_outono\\_2020.pdf](http://www.inmet.gov.br/portal/notas_tecnicas/2020/prognostico_outono_2020.pdf). Access on: 22 April, 2020.
- INMET – Instituto Nacional de Meteorologia. **Banco de dados meteorológicos do INMET (BDMEP)**. 2021. Available: <https://bdmep.inmet.gov.br/>. Access on: 19 December, 2021.
- KASTENDEUCH, P. P.; NAJJAR, G.; PHILIPS, N. Îlot de sécheresse et d'humidité à Strasbourg. **Climatology**, v. 16, p. 72-90, 2019. <https://doi.org/10.4267/climatology.1392>
- MAGHRABI, A.; DAJANI, Al H. M. Estimation of precipitable water vapour using vapour pressure and air temperature in an arid region in central Saudi Arabia. **Journal of the Association of Arab Universities for basic and applied sciences**, 14:1, 1-8, 2013. <https://doi.org/10.1016/j.jaubas.2012.11.001>
- MARINGÁ. **Lei Ordinária nº 880, de 15 de outubro de 1971**. Available: <https://leismunicipais.com.br/a/pr/m/maringa/lei-ordinaria/1971/88/880/lei-ordinaria-n-880-1971-denomina-parque-do-inga-o-bosque-dr-etelvino-bueno-de-oliveira>. Access on: 15 March, 2022.
- MARINGÁ. **Lei Ordinária nº 10.353, de 12 de janeiro de 2016**. Available: <https://leismunicipais.com.br/a/pr/m/maringa/lei-ordinaria/2016/1035/10353/lei-ordinaria-n-10353-2016-dispoe-sobre-a-oficializacao-do-parque-do-inga-prefeito-adriano-jose-valente-como-unidade-de-conservacao-na-categoria-area-de-relevante-interesse-ecologico>. Access on: 20 August, 2021.
- MELLO, Y. R. de; KOHLS, W.; OLIVEIRA, T. M. N. de. Uso de diferentes métodos para o preenchimento de falhas em estações pluviométricas. **Boletim de Geografia**, Maringá, v. 35, n. 1, p. 112-121, 2017. <https://doi.org/10.4025/bolgeogr.v35i1.30893>
- MINAKI, C.; MONTANHER, O. C. Influência do El Niño-Oscilação Sul na precipitação em Maringá-PR, no período de 1980 a 2016. **Caminhos de Geografia**, Uberlândia-MG, v. 20, n. 69, p. 266-281, mar. 2019. <https://doi.org/10.14393/RCG206941220>
- MINAKI, C.; MONTANHER, O. C. Variáveis climáticas e os registros de incêndios em Maringá-PR. **Revista Brasileira de Climatologia**, v. 27, ano 16, p. 518-538, jul/dez 2020. <http://dx.doi.org/10.5380/abclima.v27i0.74403>
- MORETTIN, P. A.; BUSSAB, W. O. **Estatística básica**. 8. ed. São Paulo: Saraiva, 2013.
- ONO, H. S. P.; KAWAMURA, T. Sensible climates in monsoon Asia. **International Journal of Biometeorology**, v. 35, n. 1, p. 39-47, 1991. <https://doi.org/10.1007/BF01040962>
- RANSOM, W. H. Solar radiation and temperature. **Weather** 8, p. 18-23, 1963. <https://doi.org/10.1002/j.1477-8696.1963.tb05137.x>
- R Core Team (2020). **R: A language and environment for statistical computing**. R Foundation for Statistical Computing, Vienna, Austria. Available: <https://www.r-project.org/>. Access on: 10 January, 2020.
- RESCHILIAN, P. R.; UEHARA, A. Y. Desafios à questão metropolitana: o processo de organização do espaço urbano e regional de Maringá. **Oculum Ensaios**, 15, Campinas, p. 76-87, jan-jun. 2012. Available: <https://periodicos.puc-campinas.edu.br/oculum/article/view/886/864>. Access on: 10 March, 2022.
- SIMEPAR – Sistema de Tecnologia e Monitoramento Ambiental do Paraná. Solicitação de dados [email]. 2021. Email received by [cminaki@uem.br](mailto:cminaki@uem.br) on: 10 October, 2021.
- SUTCLIFFE, R. C. Water balance and the general circulation of the atmosphere. **Quarterly Journal of Royal Meteorological Society**. 82, p. 385-395, 1956. <https://doi.org/10.1002/qj.49708235402>
- THOM, E. C. The discomfort index. **Weatherwise**, v. 12, n. 1, p. 57-70, 1959. <https://doi.org/10.1080/00431672.1959.9926960>
- TULLER, S. E. World distribution of mean Monthly and annual precipitable water. **Monthly Weather Review**, v. 96, n. 11, p. 785-797, nov. 1978. [https://doi.org/10.1175/1520-0493\(1968\)096<0785:WDOMMA>2.0.CO;2](https://doi.org/10.1175/1520-0493(1968)096<0785:WDOMMA>2.0.CO;2)

VIANELLO, R.L.; ALVES, A. R. **Meteorologia básica e aplicada**. 2. ed. Viçosa-MG: Ed. UFV, 2012.

WALLACE, J. M.; HOBBS, P. V. **Atmospheric Science: an introductory survey**. 2. ed. University of Washington: British Library, 2006. Available:

[https://www.academia.edu/37366881/Atmospheric\\_science\\_wallace\\_and\\_hobbs\\_PDF](https://www.academia.edu/37366881/Atmospheric_science_wallace_and_hobbs_PDF). Access on: 26 July, 2021.

WMO - World Meteorological Organization. **Guide to Meteorological Instruments and Methods of Observation**. Switzerland: WMO, 2008, n. 8. Available:

<https://www.posmet.ufv.br/wp-content/uploads/2016/09/MET-474-WMO-Guide.pdf>. Access on: 26 July, 2021.

### AUTHORS' CONTRIBUTION

Cíntia Minaki carried out the bibliographic research, analyzed the data and wrote. Vincent Dubreuil collaborated with data analysis and text review. Margarete Cristiane de Costa Trindade Amorim managed the project, supervised and revised the text.



This is an Open Access article distributed under the terms of the Creative Commons Attribution License, which permits unrestricted use, distribution, and reproduction in any medium, provided the original work is properly cited